ACS APPLIED MATERIALS & INTERFACES

RESEARCH ARTICLE

www.acsami.org

Inorganic/Organic (SiO_2)/PEO Hybrid Electrospun Nanofibers Produced from a Modified Sol and Their Surface Modification Possibilities

Georgios Toskas,*[,†] Chokri Cherif,[†] Rolf-Dieter Hund,[†] Ezzedine Laourine,[†] Amir Fahmi,[‡] and Boris Mahltig[§,#]

[†]Institute of Textile Machinery and High Performance Material Technology (ITM), Technische Universität Dresden, Hohestrasse 6, 01069 Dresden, Germany

[‡]Manufacturing Division, Faculty of Engineering, University of Nottingham, University Park, Nottingham NG7 2RD, United Kingdom

[§]Gesellschaft zur Förderung von Medizin, Bio- und Umwelttechnologien, GMBU e.V., Postfach 520165, 01317 Dresden, Germany

Supporting Information

ABSTRACT: Ceramic silica (SiO_2) hybrid nanofibers were prepared by electrospinning of solutions containing biocompatible polymer and modified silica precursors. The new hybrid nanofibers are based on polyethylene oxide (PEO) and a new solution of modified sol−gel particles of mixture containing tetraethoxysilane (TEOS) and 3-glycidyloxypropyltriethoxysilane (GPTEOS) in a weight ratio of 3:1. Adding high-molecular-weight PEO into the silica sol is found to enhance the formation of the silica nanofibers and leads to reduce the water-soluble carrying polymer down to 1.2%wt. Transmission electron microscopy (TEM) and attenuated total reflection fourier transformation infrared ATR-FTIR measurements are suggested that PEO is encapsulated by the silica component. This excellent formulation renders electrospinning of SiO_2 a robust process for an easy production of controllable silicate nanofibrous matrices. For instance, nanofibers with average diameter down to 400 nm are accessible by varying the weight ratio between the polymer and the inorganic precursor. These are reduced to 120 nm after the pyrolysis process. Moreover, the surface of the nanofibers could be easily modified, either by Al^{3+} leading to aluminium silicate coatings, or by incorporation of Ca^{2+} ions and subsequent bioactive hydroxyl carbonate apatite (HAP) formation. These hybrid silica nanofibers are possess a unique collective properties can have a great impact either in high-temperature reinforced materials and filtration or in biomedical applications such as in dentistry and bone tissue engineering.

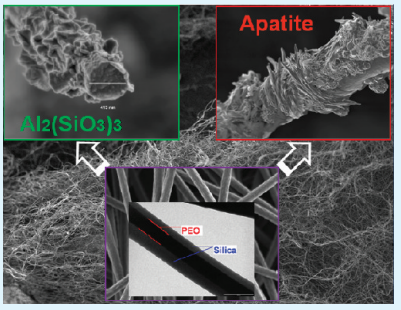

KEYWORDS: electrospinning, sol−gel, SiO_2/PEO nanofibers, Al-SiO_2, hydroxyapatite coating

INTRODUCTION

Nanocomposites are a new class of materials based on organic polymers and inorganic substances. Combining both counterparts in one material uses the advantages of the flexibility and good mold ability of the organic part, and heat stability, high strength, and chemical resistance of the inorganic part. These organic−inorganic nanocomposite materials present mean for membrane applications. In previous studies, a direct blending method of the pre-prepared nanoparticles with polymers has led to the modification of asymmetric membranes. However, this method is limited because of a lack reproducibility, whereas significant nanoparticle aggregation in the membrane casting solution and poor stability of the nanoparticles onto the membrane surfaces.[1,2] The development of sol−gel technique has provided nanosols for various surface modifications. The most investigated nanosol systems are silica sols. By hydrolyzing metal alkoxides following condensation, a dispersion of nanosized alkoxide particles is formed. The coating of this dispersion can form xerogel films after solvent evaporation.[3] This technique has offered many advantages by improving the compatibility of inorganic−organic materials without affecting the organic polymer properties.[4]

Nanofiber matrices via electrospinning have been found in a large number of applications in the industrial sector, i.e., in filtration, membrane, textile coating and catalysis and also in biomedical field, i.e., in wound healing, drug delivery systems, and tissue engineering scaffolds.[5] Electrospun nanofibers include synthetic and natural polymers, but also hybrid fibers of metal and ceramic.[6,7] A great number of electrospun ceramic nanofibers, including silica (SiO_2) and titanium (TiO_2) nanofibers, have been prepared and studied.[8−11] Silica (SiO_2) is the most convenient and widely used because of its mild reactivity and good chemical properties. The multifunction of the SiO_2 unmodified or modified nanofibers can range from resistant to corrosion and protective textiles to dental and biomedical applications. Modified SiO_2 nanofibers coated with aluminum nitride (AlN) have been proposed for photovoltaic space-based applications,[12] whereas sol−gel-derived bioactive silica glass nanofibers have been recently introduced as scaffolding matrices for bone-tissue

Received: July 1, 2011
Accepted: August 22, 2011
Published: August 22, 2011

regeneration.[13−15] Moreover, coating ability of apatite on ceramics has been known for a long time[16] and has recently been tested on silica glasses of various alkoxide systems.[13,15]

Two methods of preparing silica electrospun nanofibers via solutions (spin dopes) are frequently applied: the first method is the direct spinning of aged sol−gel solutions prepared from alkoxide precursors and the second is spinning from an organic solution containing alkoxide precursors and carrying polymers. In the first method, solid and dense fibers are obtained. But the diameters reported are of the micrometer range, down to 0.7 μm.[14] Besides, as pH and concentrations of the sol-gel constituents are the main factors influencing the gelation and the solution viscosity, the direct method is difficulty controlled. Thus, the solutions containing organic polymers are more easily adjusted, generating nanofibers of controllable size and uniformity. These ceramic nanofibers, also known as polymer-derived ceramics (PDCs), can subsequently submitted to direct thermal decomposition (pyrolysis) of the polymeric counterpart.[17] Nevertheless, it has been reported that the brittleness of the sintered ceramic nanofibers produce whiskers when broken in vivo, leading to potential carcinogenesis.[18] Therefore, for biomedical purposes, nonsintered silica/polymer composites should be preferred.

As alkoxide precursor, tetraethoxysilane (TEOS) and tetramethoxysilane (TMOS) are commonly used.[19,20] As carrying coelectrospun polymer, the most studied are polyvinyl pyrrolidone (PVP), poly(vinylidene fluoride (PVDF), nylon-6 ,and polyvinyl alcohol (PVA).[1,20,21] In regenerative medicine, the potential biomedical use of new resorbable materials is governed by the physiochemical properties, biological compatibility and by their biodegradability. The bioactive silica gel fibers that are not treated by heat have been reported to dissolve easily in vivo, whereas the silanol groups of the silicate ions are known to act as nucleation sites for the development of hydroxyapatite crystals.[22]

Herein, we have created new types of organic−inorganic composite nanofibrous membranes. They are based on one of the most used non-toxic and biocompatible polymers, polyethylene oxide (PEO).[23−25] A new organically modified alkoxide sol−gel solution is used containing a mixture of tetraethoxysilane (TEOS) and 3-glycidyloxypropyltriethoxysilane (GPTEOS) containing an epoxy group. Furthermore, epoxies as *N*,*N*-diglycidyl-4-glycidyloxyaniline (tri-epoxy)[26] or bisphenol A propoxylate diglycidyl ether[27] have been used as cross-linkers for the reinforcement of the skeletal structure of typical silica aerogels appropriate for aerospace applications.[28]

The objectives of this work were, first to obtain a controllable and easy process of silica nanofibers, and subsequently examine the effect of varying the polymer to precursor weight ratio and correlate that to the structural properties of the nanofibers. The second aim was to prove the ability of these hybrid nanofibers to modify (i) by creating aluminum silicate coatings under Al hypersaturated conditions giving rise to high temperature and nanofiltration media, (ii) by incorporating calcium ions resulting in bioactive hydroxyl carbonate apatite (HAP) crystal formation.

EXPERIMENTAL SECTION

Materials. The polyethylene oxide (PEO) used in these experiments was purchased from Sigma-Aldrich (M_v = 900 000 Da). Acetic acid was bought from Normapur (PROLABO), Germany. Deionized water was used for the preparation of solutions. Dulbecco's modified eagle's medium (DMEM - D6046), low glucose with 1000 mg/L glucose, L-glutamine, and sodium bicarbonate, liquid sterile filtered, was also purchased from Sigma, Germany.

Preparation of Electrospun Nanofibers. The modified silica sol was prepared by hydrolyzing tetraethoxysilane and 3-glycidyloxypropyltriethoxysilane in a weight ratio of 3:1. The sol was hydrolyzed in 0.01 N HNO_3 and in presence of ethanol, in a volume ratio of: (TEOS/GPTEOS):HNO_3:C_2H_5OH = 1:0.2:4.2. After being stirred for 24 h, the solution was ready for the preparation of the spin-dopes. A 3 wt % PEO solution was prepared separately in 0.5 M acetic acid and stirred for a period of 24 h. The PEO solutions were then mixed in various weight ratios with the alkoxide solution. The resultant mixtures were stirred for at least 6 h to ensure adequate mixing.

The electrospinning apparatus was set up horizontally, as it has been previously described.[29] The silica/polymer solution was put into a 1 mL disposable syringe fitted with 0.60−1.0 mm 23 gauge tip-ground-to-flat needles and fed with the help of a programmable KD scientific pump. Typical parameters operated in this study were flow rates between 0.4 and 1.0 mL/h, voltages between 28 and 30 kV and a tip to collector optimal distance of 11 cm; environmental conditions: 22 °C and RH = 55%.

Characterization of Nanofibrous Membrane. *Rheology.* A Haake MARS (Haake, Germany) stress-controlled rheometer was used for the measurements of the solutions viscosity parameters. Cone−plate geometry (35 mm radius, 2°, Ti) was used for the shear measurements and the oscillatory movement. The gap for all solutions was 0.100 mm at a temperature of 20 ± 0.1 °C.

Microscopy: Scanning Electron Microscopy-EDX; Transmission Electron Microscopy. A DSM 982 Gemini (Zeiss, Germany) Scanning Electron Microscope served for the examination of the morphology of the nanofibers. The as-spun nanofibers were dried under vacuum at room temperature and sputter-coated with silver/graphite. The samples were examined at an accelerating voltage of 1.0 kV and magnifications from 200 to 50000. The SEM images were then used to evaluate the fiber diameter. The average fiber diameter was determined using Digital Image Processing System 2.6 (point electronic GmbH) software in conjunction with the SEM image. Ten different fiber diameters were determined and averaged to find the fiber diameter reported for each of the resulting electrospun mats. The 95% confidence limits of the mean were calculated and reported with each average fiber diameter.

For the transmission electron microscopy (TEM), the samples were deposited as received in copper TEM grids carbon-coated copper grids (400 meshes, AGAR Scientific). Transmission electron microscope (TEM) from TECNAI Biotwin (FEI Ltd.) at 100 keV was used to observe the samples. Any treatment has been performed on the microfibers to avoid any deterioration of the samples.

Infrared Spectroscopy. IR spectra were obtained by using the attenuated total reflection (ATR) method on a FTIR Bruker Tensor 27 spectrophotometer.

Bioactivity Test. For the development of apatite nucleation sites on the hybrid silicate nanofibers, CaO in the form of calcium chloride dihydrate was added in the initial sol-gel solution, before electrospinning. The molar ratios of $CaCl_2 \cdot 2H_2O$, GPTEOS, TEOS, ethanol, HNO_3, and water were 0.08:0.2:0.6:13.5:0.004:1.9, respectively. The bioactivity of the as-obtained nanofibers were assessed for their apatite forming ability in modified simulated body fluid (m-SBF) according to Oyane et al (see the Supporting Information, Table 1).[30] The specimens of 10 mg were placed in a Petri glass disk and immersed in 10 mL of m-SBF solution buffered at pH 7.4 for up to 7 days without refreshing. The temperature was held at 37 °C through gentle stirring. After being soaked, the samples were carefully rinsed with deionized water and dried at room temperature.

RESULTS AND DISCUSSION

Properties of Solutions. Nanofibrous membranes were prepared by electrospinning starting from an organically modified

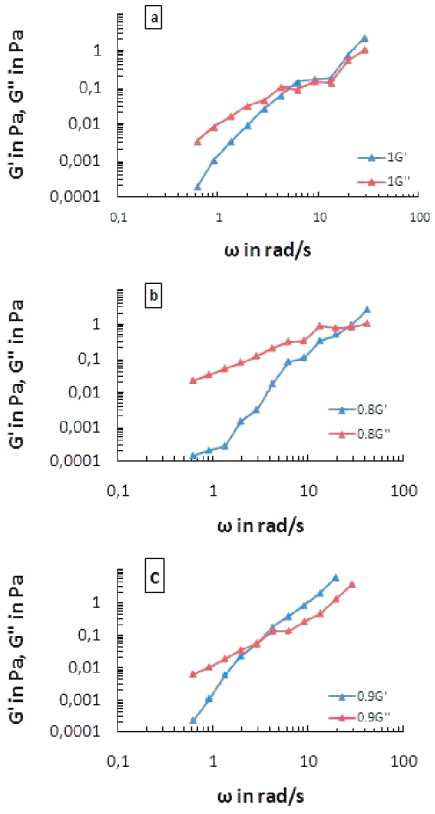

Figure 1. Effect of silicate content according to PEO addition in sol−gel solution on storage (G') and loss (G'') moduli as function of frequency at 20°C: (a) SiO_2 sol−gel, (b) SiO_2/PEO 80/20 wt, (c) SiO_2/PEO 90/10 wt. The 1, 0.8, and 0.9 represent the weight ratio of silicate to the final spin dope.

silica sol. Organosilanes as used for the modification of silica are molecules that consist of inorganic and organic functional moieties, having the ability to bond to inorganic and organic chains, respectively. The epoxy groups of the organosilane glycidyloxypropyltriethoxysilane (GPTEOS) are susceptible of van der Waals or even covalent bonding, through nucleophilic addition. Under acidic conditions the nucleophilic, such as the CH_3COO^- derived from acetic acid in the PEO solution, attacks the carbon to form stable carbocation, i.e. the most substituted carbon, leading to the epoxide ring-opening. Organic domains can be formed through this organic functionality, whereas more hydroxyl (−OH) groups are formed for hydrogen and ionic bonding. The mixture of silanes, tetraethoxysilane and 3-glycidyloxypropyltriethoxysilane in a weight ratio of 3:1 was attempted to electrospin either as-prepared or after ageing at 80°C for 2 h. After ripening a solution having a dynamic viscosity of 11 mPa·s, electrospinning resulted only in nanodroplet formation through electrospraying (see the Supporting Information, Figure 1). Therefore, a co-blending polymer had to be added to the as-prepared alkoxide solution in order to regulate the viscoelastic parameters, necessary for the nanofiber production. Polyethylene oxide (PEO) was chosen as a biocompatible polymer. Several trials were performed with PEO, by varying polymer to alkoxide precursor weight ratio. The minimum concentration of the carrying polymer, capable of producing nanofibers was selected and used. Thus, only 3 wt % PEO was used as blending polymer solution, even if PEO sole is giving at this concentration beaded nanofibers (see the Supporting Information, Figure 1).

Table 1. Variation of pH and Dynamic Viscosity (η_{dyn}) as to SiO_2/PEO Weight Ratio

SiO_2/PEO wt	pH	η_{dyn} (mPa s)
100 (SiO_2)	3.7	5
1/100 (PEO)	2.9	407
50/50	3.9	230
80/20	4.6	85
90/10	4.8	56
96/04	4.9	50

The viscosity of polymer solutions is related to the intermolecular interactions among the polymer chains. The initial dynamic viscosity of 3 wt % PEO used in this study was measured 407 mPa s, whereas that of 4 wt % PEO giving un-beaded nanofibers was 1550 mPa s. In addition, the initial dynamic viscosity measurement (η_{dyn}) of the silane solution, designated hereafter as SiO_2, is found to be only 5 mPa s. A net decrease in viscosity is observed with the addition of the sol (see Table 1). Markedly, solutions of sol−gel systems with such low viscosities down to 50 mPa s can successfully electrospin.[12]

The conductivities of the spin-dopes are governed by the PEO solution conductivity, measured 1350 μS/cm, and decreased down to 5.5 μS/cm for the SiO_2/PEO 96/04 wt. solution. Hence, electrospinnability of this hybrid system is influenced by the solution surface tension. This is lowered by gradual addition of the alkoxide solution, containing about 87% w/v ethanol (surface tension of γ = 22.3 mN/m), to the aqueous PEO solution (H_2O γ = 72 mN/m).[31]

The interaction between biopolymer-silicate hybrid materials is affected by the nature of these constituents. It has been reported that in neutral pH conditions, silicates bear silanol (Si−OH) and silanolate (Si−O^-) groups, while decreasing the pH to slightly acidic (pH 4−5), the number of the negative charge of silicates is reduced and as a consequence their reactivity also decrease.[32] Therefore, the possible interaction between PEO and the sol−gel alkoxide is considered mainly through hydrogen bonds.

In parallel, it was found that other rheological factors such as an enhanced entanglement also play a significant role. In our experimental spin dopes, it was found that the loss modulus was greater than the elastic modulus ($G'' > G'$) at low frequencies (see Figure 1). Both moduli are frequency-dependent and increase in a parallel manner for PEO up to 20 Pa at an increasing frequency of oscillation. No crossover was marked for the 3% wt. PEO or for the SiO_2/PEO 50/50 wt. (results not presented). On the contrary, a crossover is observed in the initial sol−gel solution ($G' = G''$ = 0.095 Pa) at 0.85 Hz, even if the low viscosity did not permit a successful electrospinning (Figure 1a). At low frequencies, G'' is always dominating G' (G'' > G') for the SiO_2/PEO spin dopes with weight ratios of over 80/20 (Figure 1b and c). This is typical for an entangled solution.[33] Moreover, for the SiO_2/PEO 80/20 wt. ratio, a crossover occurs ($G' = G''$ = 0.58 Pa) at 3.5 Hz and from that point on at higher frequencies, the elastic modulus (G') dominates G'' (Figure 1b). Hereafter, when the silica content increased from 80% to 90 wt %, the crossover frequency is observed at lower frequencies and has moved to a decreased value of 1.2 Hz. (Figure 1c). In this case, the crossover is observed at $G' = G''$ = 0.17 Pa. This shift of the crossover point has been correlated with the effective

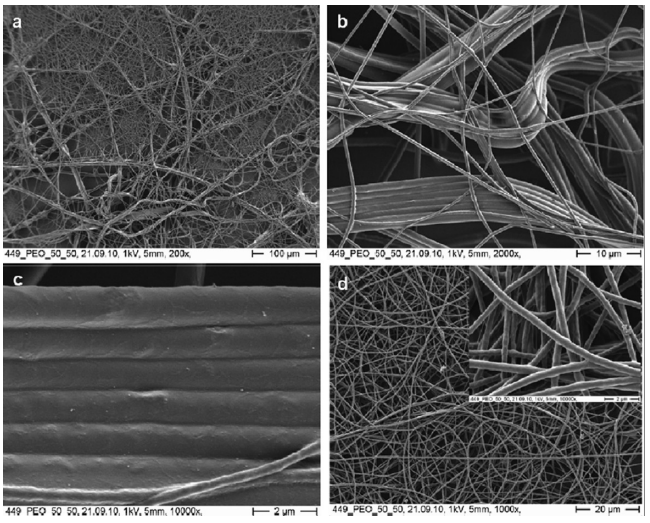

Figure 2. SiO_2/PEO electrospun micro- and nanofibers from 50/50 weight ratio.

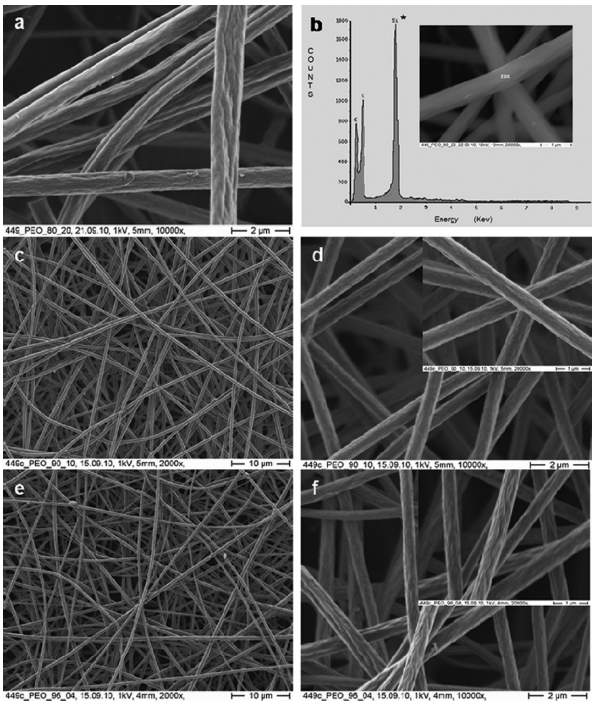

Figure 3. (a) SiO_2/PEO electrospun nanofibers from 80/20 weight ratio and (b) the respective EDX spectrum, (c, d) 90/10 and (e, f) 96/04 weight ratios.

crosslinking change or chain entanglement, thus with the higher electrospinning ability of a polymer solution.[29,33,34] Strong hydrogen bonding among the silicate and PEO polymer chain are considered to be at the origin of this enhanced entanglement.

Morphology/Structural Properties of the Nanofibers. To study the effect of polymer to alkoxide precursor variation, we tested full weight ratio margins by using PEO as carrying polymer system. The focus was on the production of uniform nanofibers. With SiO_2/PEO solutions in which polyethylene oxide was overlying 50 wt %, two populations of fibers consisting of micro- and nanofibers are formed (see Figure 2). Thus, the microfiber

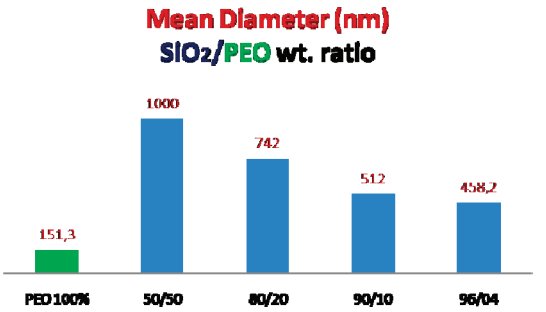

Figure 4. Effect of polymer (PEO) weight ratio on fiber diameter.

part of the membrane consists of fibers with an average diameter of 1000±8 nm and the nanofiber part has fibers ranging from 357−274 nm with a mean diameter of 315±38 nm. This result is also reflected in ATR-FTIR spectrum (Figure 7c) where the assignments of both components are observed. The formation of silicate microfibers together with PEO nanofibers cannot be excluded. This even if the average diameter of the PEO nanofibers electrospun alone was found 151±23 nm, which means half of the previously obtained by the mixed SiO_2/PEO 50/50 wt % solutions.

With SiO_2/PEO solutions of 80/20 wt, 90/10 wt, and 96/04 wt, nanofibers with average diameters of 744 ± 139 nm, 512 ± 31 nm and 458 ± 43 nm are produced, respectively (see Figures 3 and 4). This shows that only 4 wt % PEO as the weight ratio of the 3 wt % added to silica oxide (96 wt %) is providing a functional system able to produce uniform nanofibers. Thus, 1.2 wt % total PEO is the minimum amount required for the continuous fiber production. Silicon is detected by EDX on the fiber surface of all samples (Figure 3b). Nonetheless, these fibers show relatively rough surfaces, when electrospun on a stable collector. The wrinkled fiber surfaces imply the competition between the phase separation dynamics and the fast evaporation rate of solvents (in our case, ethanol/H_2O) during electrospinning.[35] As spinning voltage, temperature and relative humidity were kept fixed, only the polymer/solvent properties could influence the fiber morphology. Thus, the PEO content and the solvents' relative vapor pressures (C_2H_5OH: 43.89 mmHg/20 °C; H_2O: 17.54 mmHg/20 °C) can alter the nanofiber roughness. An increase in roughness is achieved under (i) an increase in the solvent vapor pressure induced by the silica component, (ii) a decrease in the ethylene units in the hybrid nanofibers.

The nanofiber diameters measured with this system are about 3−5 times enlarged by increasing the polyethylene oxide content, compared to PEO nanofibers of average diameter 151 ± 23 nm (Figure 4).

Furthermore, one could expect an increase of the average diameters at elevated SiO_2 ratio as diameters of silica nanofibers reported in literature are found to be at the range of 1 μm.[21,36] The opposite phenomenon observed in our experiments could be attributed: (i) to the viscosity reduction, from 230 mPa s for SiO_2/PEO 50/50 wt to 50 mPa s for the 96/04 wt ratio and (ii) hydrogen bonding, among the hydrolyzed by the moisture in atmosphere silica and polyethylene oxide. The excellent electrospinnability of the investigated formulation was further proved by the use of a rotating collector with a 4 mm diameter. At a rotational speed of 100 rpm, a solution of SiO_2/PEO 90/10 wt produced a nanofiber mat of about 100 μm thickness in relatively short time scale of 20 min. The nanofibers produced with this

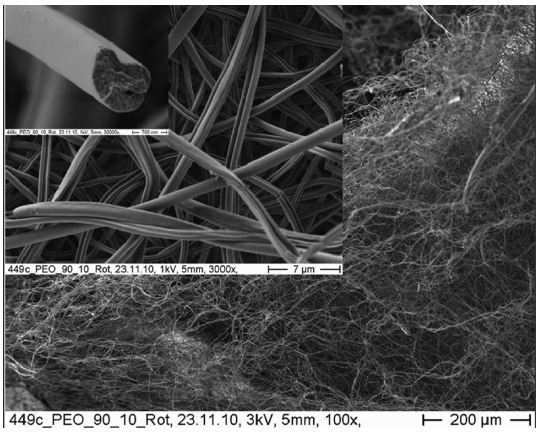

Figure 5. Nanofibers collected with a rotating collector: Sigmoid morphology.

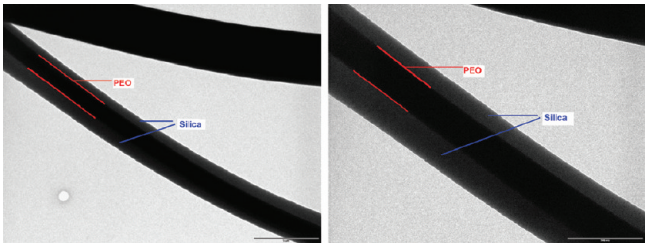

Figure 6. TEM micrograph revealing the core−shell structure of SiO_2/PEO 90/10 wt. nanofibers.

method, presented smooth surfaces and a sigmoid-curved morphology (see Figure 5). The smooth surfaces are resulting from the uniaxial extension of the jet in the electric field, whereas the sigmoid morphology can arise from the free charges on the nanofiber surface and the sudden stretch caused by the rotation, thus leading to a longitudinal bending of the fibers.

The inner morphology of nanofibers was determined by transmission electron microscopy (TEM). For the nanofibers composed of up to 20 wt % polyethylene oxide, no obvious phase partitioning between the two phases, PEO and silica, is observed (see the Supporting Information, Figure 2). Nevertheless, silicon was always detected by EDX and ATR-FTIR on the fiber surface (Figures 3b and 7d). In the samples with a weak PEO ratio of less than 10% wt., the difference of contrasts indicates that the fibres are composed of two distinctly partitioned materials in a core-shell structure. Figure 6 shows the TEM micrographs of SiO_2/PEO 90/10 wt. nanofibers. In this case, it is suggested that polyethylene oxide is encapsulated by the silicate component. The initially incorporated epoxy silane (GPTEOS) is considered to provide a more flexible silica backbone through the alkyl-linked organic domains and a larger amount of hydroxyl groups contributing to the hydrogen bonding with the slightly negative PEO oxygen. When the relative PEO mass is much inferior (less than 10 wt %) to the silica component, a complex phase separation can occur leading to PEO inclusion. As ethanol is rapidly evaporated when the hybrid material is ejected, the decrease of temperature at the fiber surface is important, resulting in thermally induced phase separation.[37] The reduction of this temperature can vary for the two components, introducing diverse free energy surfaces and leading to a self assembled structure.

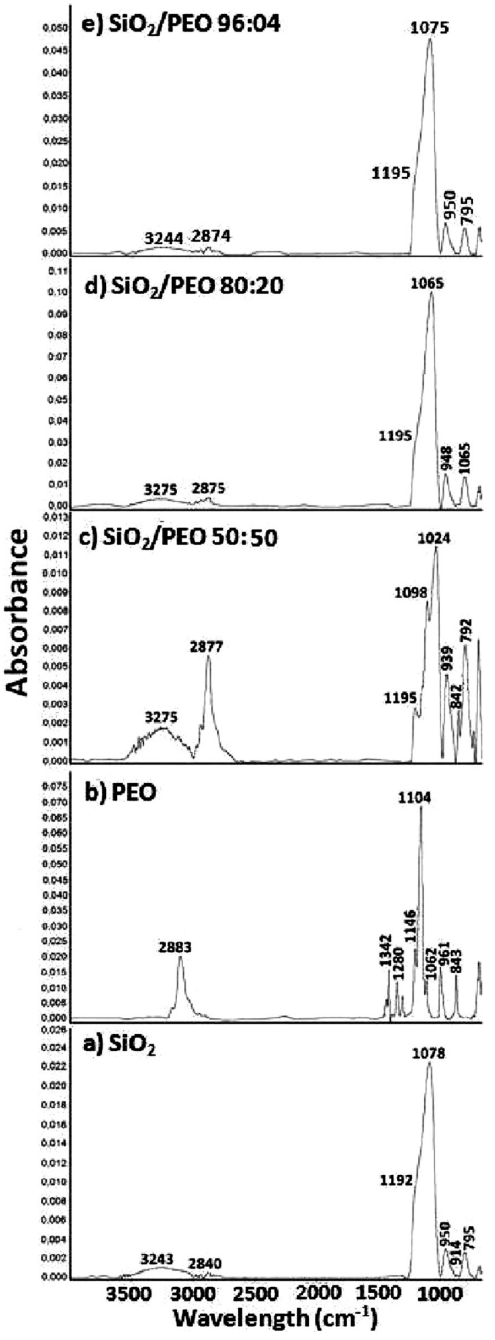

Figure 7. ATR-FTIR spectra of (a) SiO_2 (TEOS/GPTEOS), (b) PEO, (c) SiO_2/PEO (50:50), (d) SiO_2/PEO (80:20), and (e) SiO_2/PEO (96:04).

Fiber Composition. The phase composition of the hybrid fibers was confirmed by ATR-FTIR spectra. Figure 7a is presenting the FTIR spectrum of the TEOS/GPTEOS (designated as SiO_2) nanoparticles electrosprayed from the initial alkoxide solution. The wide peak in the range of 3300−3700 cm^{-1} is assigned to the hydroxyl stretching of the silanol groups. In the same spectrum, the characteristic bands of silica xerogel are observed: those at 1078 and 950 cm^{-1} and 795 cm^{-1} are attributed to Si−O−Si and Si−OH stretching vibrations, respectively.[38] In the stronger peak of 1078 cm^{-1}, a shoulder at about 1192 cm^{-1} is attributed to the presence of epoxy group from

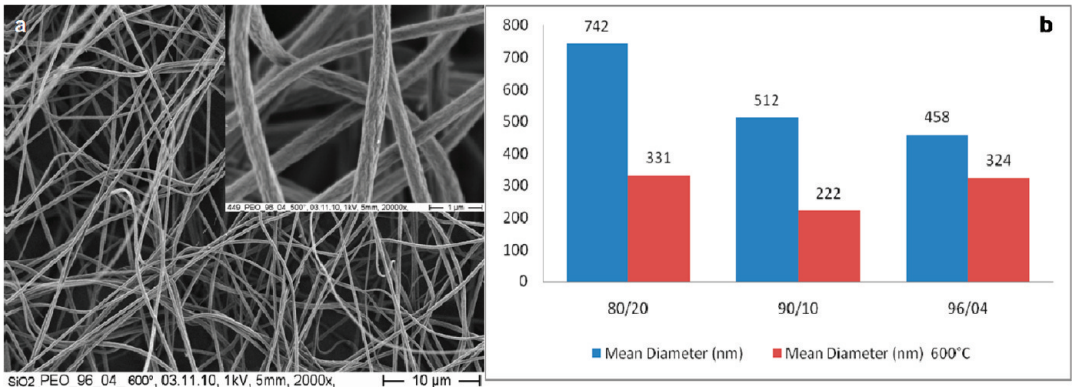

Figure 8. Effect of pyrolysis: (a) on SiO_2/PEO (96/04) nanofiber morphology (magnification 2000×; insert photo: magnification 20 000×) and (b) on nanofiber diameters of various SiO_2/PEO weight ratios.

the 3-glycidyloxypropyltriethoxysilane. A smaller assignment at about 2840 cm^{-1} can be attributed to the ethoxy group ($-OCH_2CH_3$). In Figure 7b, a typical ATR-FTIR spectrum of PEO electrospun nanofibers is demonstrated. The medium band at 2883 cm^{-1} and the strong triplet band at 1147, 1104, and 1062 cm^{-1} with a maximum at 1104 cm^{-1} are attributed to the C−H stretch and C−O−C accordingly. The bands assigned to the C−H wagging at 1342 cm^{-1}, C−H twist at 1280 cm^{-1}, and C−H rocking at 961 and 844 cm^{-1} are also observed.

When the modified silica sol is mixed with PEO at a ratio of 50/50 wt %, all assignments of PEO are found together of those of silanes on electrospun nanofibers. In Figure 7c, the peak at 3275 cm^{-1}, assigned to the silanol hydroxyl groups, and the medium assignment PEO at 2877 cm^{-1} characteristic of the $\nu(CH_2)$ of PEO are strongly present.[39] The strong peak of PEO assigned to C−O−C stretching, has shifted to lower wavelengths with a maximum of 1024 cm^{-1}. This peak is superposed with the Si−O−Si stretching assignment of silica at 1078 cm^{-1}. The medium secondary band at about 1195 cm^{-1} indicates the presence of an epoxy group from the 3-glycidyloxypropyltriethoxysilane. The silane assignments at about 940 and 793 cm^{-1} ascribed to the Si−O−Si and Si−OH stretching vibrations, respectively, are also observed. It should be expected that the Si−O−Si vibrations result from the volume of the former SiO_2 particles and the Si−OH vibrations are related to the surface of those particles. At higher SiO_2/PEO weight ratios of more than 80/20 wt, the FTIR spectra resemble that of alkoxide alone (Figure 7d,e). The Si−O−Si stretching assignment of silica at 1065-1075 cm^{-1} is probably superposed and merged with that of PEO assigned to C−O−C stretching. Besides, only a weak band at 2875 cm^{-1} resulting eventually from ethoxy groups of GPTEOS is observed. This indicates that most of the ethoxy groups are hydrolyzed to silanol groups (Si−OH) as implied by the broad band at 3275−3244 cm^{-1}. These hydroxyl groups are mostly found on the electrospun silicate component surface.

FTIR results showing interactions at the molecular level are consistent with new fiber complex formations. As assisted by the TEM micrographs, ATR-FTIR spectra clearly prove that PEO, in higher SiO_2/PEO weight ratios, is coated by the silicate component.

Effect of Pyrolysis/Integrity in Water. To examine the behavior on removing the carrying polymer, the nanofibers were pyrolized at 600 °C. The pyrolysis temperature was attained at 10°C/min and maintained for 2 h in order to decompose PEO.

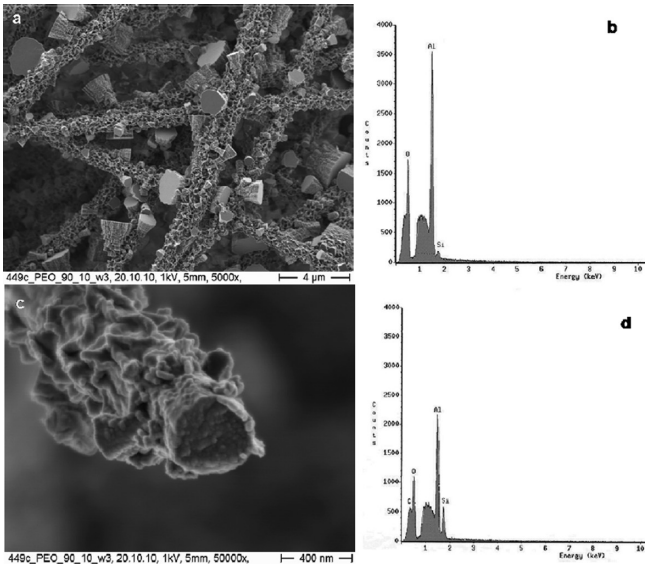

Figure 9. Aluminium silicate coating on SiO_2/PEO nanofibers after immersion in DMEM for 7 days. (a) SiO_2/PEO (90:10) nanofibers (magnification 5000×), (c) single nanofiber of ~400 nm diameter (magnification 50 000×) and their respective coatings EDX spectra.

A decrease rating from 55 to 33% on the nanofiber diameters was observed for the SiO_2/PEO system, providing nanofibers with average diameter of 222 ± 104 nm and a distribution of 400−120 nm. The fibers retain their morphology to a great degree (Figure 8), although in some experiments, they were broken into shorter segments.

PEO has a high solubility in water, and electrospun pure PEO fibrous membranes dissolve quickly in water at 37 °C. Thus, it is of practical interest to study the effect of the amount of PEO in SiO_2/PEO nanofibers on the integrity of the nanofibrous structure in water. A contraction of 59.4% on the fiber diameter is observed for the SiO_2/PEO (80/20) after immersing in deionized water at 37 °C for 48 h. Nanofibers present rough surfaces, the contraction remaining at the same levels for the following 5 days (see the Supporting Information, Figure 3). In fact, the diameter regression in water is comparable to that noted by the pyrolysis process, being 55% for the same sample. Conversely, for the SiO_2/PEO (90/10) samples where PEO was found coated by the silicate component, only a 2.5% fiber contraction

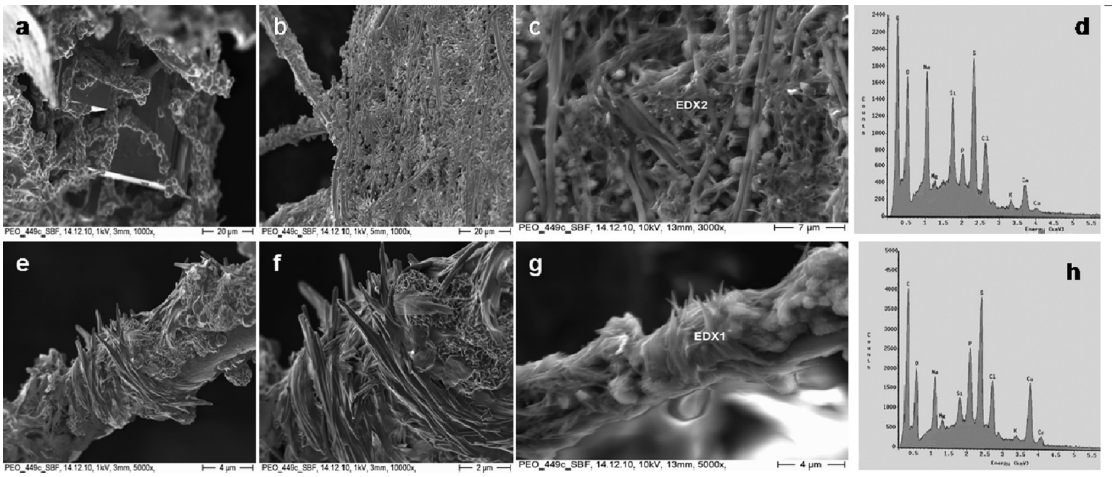

Figure 10. Hydroxyapatite formation on CaO-SiO_2/PEO nanofibers after immersion in m-SBF for 7 days. (a−c) Formation of silicate dense layer of apatite nuclei; (e−g) needlelike apatite on single nanofiber, and (d, h) EDX spectra of the hydroxyapatite formation on respective areas (c and g).

was measured after 48 h. It is suggested that the silicon oxide network of the silicate shell component is forming a hydrophobic barrier in its matrix, inhibiting water molecules from penetrating inside the fiber.

Surface Modifications. *Aluminium Silicate Coating.* Aluminium silicates, which are known to have a Mohs hardness of 4.5−7.5, are considered for insulation applications. A sample of SiO_2/PEO (90/10) was left on the aluminum foil electrospinning support and immersed in a solution of Dulbecco's modified eagle's medium (DMEM), low glucose (1.0 g L^{-1}) with a pH of 7.5, at 37 °C for 7 days. A degradation of the aluminum foil occurred, releasing Al^{3+} ions. Under Al hyper-saturated conditions, aluminium ions have created characteristic orthorhombic aluminium silicate crystals (Figure 9). Aluminium silicate is described under the general chemical formula $Al_2(SiO_3)_3$. It is known that silicic acid $Si(OH)_4$ (aq), which results during the sol−gel hydrolysis process, interacts with aqueous Al^{3+} and can reduce the bioavailability and hence the toxicity of the latter.[40] $Si(OH)_4$ is an effective scavenger of cytotoxic Al^{3+} at physiological pH. It is obvious that the efficacy of oligomeric Si^{4+} as an Al^{3+} scavenger is much greater than that of the monomer. Thus, even if silicic acid ($Si(OH)_4$) is isoelectronic with $[Al(OH)_4]^-$, as "Si^{4+}" is smaller than "Al^{3+}", the higher charge-to-radius ratio results in a greater acidity for the neutral $Si(OH)_4$ than for the anionic aluminate. Therefore, in alkaline solutions as in DMEM, $Si(OH)_4$ is found deprotonated to various degrees, whereas $[Al(OH)_4]^-$ is not.[41] The crystallization mode and complexation mechanism of Al^{3+} with silicate nanofibers need further studies which exceed the scope of the here presented work. EDX analysis of the orthorhombic crystals outside the fibers show that silicon (Si) is incorporated within the crystal structure, even in a smaller amount than in the fiber coating (Figure 9). The Al-coated SiO_2/PEO nanofibers as such can introduce applications in technical textiles and filtering. If modified by an elastomer (i.e., PDMS),[42] they can find possible application in hybrid reinforcing materials for flexible insulation.

Bioactivity (mineralization in SBF). The ability of the silanol groups on silicate ions to act as a nucleation site to form apatite crystals has been the matter of extensive investigations.[43−45] Hydroxyapatite (HAP, $[Ca_{10}(PO_4)_6(OH)_2]$) and similar calcium phosphates possess bioactive properties as to its chemical resemblance to human bones. These calcium phosphates can promote new bone formations when implanted in defected sites. In vitro investigations are simplified by the use of a simulated body fluid (SBF).[22] SBF of various types have been used for the in vitro assessment of the bioactivity of artificial materials, including silicates, and for the formation of bonelike apatite on these substrates.[13,46] The modified simulated body fluid, m-SBF has the advantages of having ion concentrations equal to those of blood plasma and being stable for a long time stored at 5 °C. In our study, the concentration of HCO_3^- is decreased to the level of saturation with respect to the calcite ($CaCO_3$) phase.[30] The introduction of CaO in the initial sol-gel solution, before electrospinning, is necessary for the development of apatite nucleation sites. In fact, the nanofibers electrospun without the addition of calcium chloride dehydrate showed very little ability of HAP formation (see the Supporting Information, Figure 4). On the contrary, the introduction of only 1.19 wt % CaO to the SiO_2/PEO (90:10) solution was proved sufficient for the apatite development on the nanofibers. This CaO incorporated percentage is immensely lower than that of up to 25−30% introduced in previous studies.[13,15] When incubated for 7 days, the fiber mat is covered with a dense layer of apatite nuclei, whereas in some of the fibers, sharp needlelike HAP has been developed as shown by SEM images (see Figure 10a−c and e−g). The large surface area of the SiO_2/PEO nanofibers results to fast HAP crystal nucleation. In general, the morphology of calcium phosphate nanoparticles has been reported needlelike, sheetlike, or spherical. Thereby, the crystals observed in Figure 10a can be attributed to the calcium precipitated as nanocrystalline phase as earlier identified (also see the Supporting Infromation, Figure 5).[14] But the formation of a magnesium (Mg) silicate monoclinic crystal or that of magnesium-substituted calcite is also possible.[47]

The EDX spectroscopy analysis, on a single fiber (Figure 10) reveals a Ca/P coating ratio of 1.54, slightly lower but close to the stoichiometry of hydroxyapatite (Ca/P = 1.67). This ratio has often been reported in carbonated apatites produced by this biomimetic process and is more similar to that of bonelike minerals.[13,45,48] Moreover, carbonate ions have shown to replace the hydroxyl or phosphate ions in the apatite crystal lattice.[49]

The major elements of mineralized nanofibrous scaffold confirmed the presence of the ions used for the m-SBF composition. Carbon (C) could also result from the sputtering of the pellets to

provide the surface conductivity for SEM observation, but silicon (Si) is still present due to the large amount of silanol groups on the nanofiber surface. The silicon peak in the EDX spectrum taken on the rough mat apatite area is larger than on single nanofiber, reflecting the non reacted silica. The observed strong peak of sulfur (S) can be attributed to the large amount (17.892 g L^{-1}) of 2-(4-(2-hydroxyethyl)-1-piperazinyl) ethanesulfonic acid (HEPES), introduced in m-SBF.[30] The mechanism of apatite formation in SBF, is a complex heterogeneous nucleation which involves: the exchange of alkali ions (Ca^{2+}, Na^{+}, K^{+}, and Mg^{2+}) with H_3O^{+} and the silanol groups (Si−OH), present through the sol-gel system, inducing $Ca_3(PO_4)_2$ nucleation via precipitation of Ca^{2+} and PO_4^{3-} and also CO^{3-}.[50,51] Thus, the crystallization of HAP occurs via dissolution of Ca, P, and Si from the nanofiber network, followed by the precipitation of Ca−P crystals from the hypersaturated SBF medium.

On the contrary to what has been observed with other composites where the inorganic phase is enclosed by the organic phase,[52] the major advantage of our hybrid system is that, the inorganic silica component is encapsulating polyethylene oxide. As a consequence, the inorganic component is directly reacting with the SBF solutes. There is also no need of fiber thermal treatments/sintering for the elimination of the organic polymer, avoiding thus carcinogenesis concerns in biomedical applications. These HAP-coated silica nanofibrous membranes can find a direct application in dentistry, i.e., for the periodontal tissue reconstruction.

CONCLUSION

Polymer-derived ceramic nanofibers have been successfully produced by the use of a new modified silica sol prepared from (TEOS/GPTEOS) and PEO as the organic carrying polymer. A highly productive electrospinning process is run to form self assembled core−shell structured nanofibers, requiring only a small amount of PEO, down to 1.2 wt % into the sol−gel solution. Major advantage of the prepared nanofibers is that we can handle the gelation chemistry and polymer addition so that all reagents are mixed from the beginning. The wrinkled morphology of the as-spun nanofibers generates a higher specific area which is a useful guideline for developing high-value-added products. The multivalent nanofibers we report here can retain their integrity in water and in bio-organic liquids as DMEM or SBF are easily modified.

The silica nanofibrous membranes can act as a scavenger reducing the cytotoxic Al^{3+}, finding thus filtration applications. Aluminium silicate was formed under alkaline conditions in DMEM. A selective Al coating could also give rise to thin sheet patterns for space insulation systems. Furthermore, novel hybrid nanofibrous matrices can rise through chemical functionalization, meeting with applications where flexibility is of importance.

The non-sintered silica/polymer composites are considered non carcinogenic. Hydroxyapatite/silica nanocomposites have been found promoting new bone formation when implanted in vivo. The SiO_2/PEO nanofibers we have fabricated have shown an excellent bioactivity in m-SBF, coated by hydroxyl apatite crystals. Therefore, these nanofibrous membranes are proving to be a good non-toxic and bioactive material for biomedical applications, i.e., dental and bone tissue regeneration or drug release through their core−shell structure.

Ongoing research is currently being conducted to unveil the functionalization possibilities and mechanical properties of the structured composite systems.

ASSOCIATED CONTENT

Supporting Information. Table on chemical composition of modified simulated body fluid (M-SBF), and five supporting in-detail figures. This material is available free of charge via the Internet at http://pubs.acs.org.

AUTHOR INFORMATION

Corresponding Author

*Tel.: +49 351 46342244. Fax: +49 351 4634026. E-mail: Georgios.Toskas@tu-dresden.de.

Present Addresses

[#]University of Applied Sciences, Faculty of Textile and Clothing Technology, Webschulstrasse 31, 41065 Mönchengladbach, Germany.

ACKNOWLEDGMENT

The authors dedicate this article to Professor Mr. Horst Böttcher on his retirement and thank him for the fruitful discussions. They also thank Mr. Axel Mensch, responsible for the SEM laboratory of the Institute of Materials Science of the Technical University of Dresden (TUD), and his collaborators Mrs. Silvia Muehle and more specially Mrs. Ortrud Trommer for their invaluable help; also Dr. Sascha Heinemann of the Max Bergmann Center of Biomaterials (TUD) for the elaboration and kind supply of the m-SBF solution, and Mrs. Martina Dziewiencki (ITM/TUD) for the FTIR measurements. In addition, the authors thank Mrs. Daniela Heinrich and Mr. Alaa Abd Elkhalek for the technical assistance.

REFERENCES

(1) Kim, Y.-J.; Ahn, C. H.; Choi, M. O. *J. Eur. Polym.* **2010**, *46*, 1957–1965.
(2) Bottino, A.; Capannelli, G.; D'Asti, V.; Piaggio, P. *Sep. Purif. Technol.* **2001**, *22*, 269–275.
(3) Mahltig, B.; Textor, T. In *Nanosols and Textiles*; World Scientific Publishing: Singapore, 2008; p12.
(4) Cho, J. W.; Sul, K. I. *Polymer* **2001**, *42*, 727–736.
(5) Greiner, A.; Wendorf, J. H. *Angew. Chem.* **2007**, *46* (30), 5670–5703.
(6) Bognitzki, M.; Becker, M.; Graeser, M.; Massa, W.; Wendorff, J. H.; Schaper, A.; Weber, D.; Beyer, A.; Gölzhäuser, A.; Greiner, A. *Adv. Mater.* **2006**, *18*, 2384–2386.
(7) Agarwal, S.; Wendorff, J. H.; Greiner, A. *Macromol. Rapid. Commun.* **2010**, *31*, 1317–1331.
(8) Sigmund, W.; Yuh, J.; Park, H.; Maneeratana, V.; Pyrgiotakis, G.; Daga, A.; Taylor, J.; Nino, J. C. *J. Am. Ceram. Soc.* **2006**, *89* (2), 395–407.
(9) Li, D.; McCann, J. T.; Xia, Y. *J. Am. Ceram. Soc.* **2006**, *89* (6), 1861–1869.
(10) Sundarrajan, S.; Richard Chandrasekaran, A.; Ramakrishna, S. *J. Am. Ceram. Soc.* **2010**, *93* (12), 3955–3975.
(11) Dai, Y.; Liu, W.; Formo, E.; Sun, Y.; Xia, Y. *Polym. Adv. Technol.* **2011**, *22*, 326–338.
(12) Zhang, G.; Kataphinan, W.; Teye-Mensah, R.; Katta, P.; Khatri, L.; Evans, E.A.; Chase, G.G.; Ramsier, R.D.; Reneker, D.H. *Mater. Sci. Eng., B* **2005**, *116*, 353–358.
(13) Kim, H.-W.; Kim, H.-E.; Knowles, J.C. *Adv. Funct. Mater.* **2006**, *16*, 1529–1535.

(14) Seol, Y.-J.; Kim, K.-H.; Kim, I. A.; Rhee, S.-H. *J. Biomed. Mater. Res., A* **2010**, *94* (2), 649–659.
(15) Poologasundarampillai, G.; Ionescu, C.; Tsigkou, O.; Murugesan, M.; Hill, R. G.; Stevens, M. M.; Hanna, J. V.; Smith, M. E.; Jones, J. R. *J. Mater. Chem.* **2010**, *20*, 8952–8961.
(16) Kokubo, T. *J. Non-Cryst. Solids* **1990**, *120*, 138–151.
(17) Sarkar, S.; Chunder, A.; Fei, W.; An, L.; Zhai, L. *J. Am. Ceram. Soc.* **2008**, *91* (8), 2751–2755.
(18) Johnson, N.; Hahn, F. *Occup. Environ. Med.* **1996**, *53*, 813–816.
(19) Choi, S.-S.; Lee, S. G.; Im, S. S.; Kim, S. H.; Joo, Y. L. *J. Mater. Lett.* **2003**, *22*, 891–893.
(20) Shao, C.; Kim, H.-Y.; Gong, J.; Ding, B.; Lee, D.-R.; Park, S.-J. *Mater. Let.* **2003**, *57*, 1579–1584.
(21) Liu, Y.; Sagi, S.; Chandrasekar, R.; Zhang, L.; Hedin, N. E.; Fong, H. *J. Nanosc. Nanotechn.* **2008**, *8*, 1528–1536.
(22) Kokubo, T; Kushitani, H.; Sakka, S.; Kitsugi, T.; Yamamuro, T. *J. Biomed. Mater. Res.* **1990**, *24*, 721–734.
(23) Bhattarai, N.; Edmondson, D.; Veiseh, O.; Matsen, F. A.; Zhang, M. *Biomaterials* **2005**, *26*, 6176–6184.
(24) Jayakumar, R.; Prabaharan, M.; Nair, S.V.; Tamura, H. *J. Biotech. Adv.* **2010**, *28*, 142–150.
(25) Toskas, G.; Laourine, E.; Kaeosombon, W.; Cherif, C. *International Conference on Latest Advancements in High Tech Textiles and Textile-Based Materials*; Ghent, Belgium, Sept 23−25, 2009; Universiteit Gent: Gent, Belgium, 2009.
(26) Meador, M. A. B.; Fabrizio, E. F.; Ilhan, F.; Dass, A.; Zhang, G.; Vassilaras, P.; Johnston, J. C.; Leventis, N. *Chem. Mater.* **2005**, *17*, 1085–1098.
(27) Meador, M. A. B.; Scherzer, C. M.; Vivod, S. L.; Quade, D.; Nguyen, B. N. *ACS Applied Mater. Interfaces* **2010**, *2*, 2162–2168.
(28) Randall, J. P.; Meador, M. A. B.; Jana, S. C. *ACS Applied Mater. Interfaces* **2011**, *3*, 613–626.
(29) Toskas, G.; Hund, R. D.; Laourine, E.; Cherif, C.; Smyrniotopoulos, V.; Roussis, V. *Carbohyd. Polym.* **2011**, *84*, 1093–1102.
(30) Oyane, A.; Kim, H.-M.; Furuya, T.; Kokubo, T.; Miyazaki, T.; Nakamura, T. *J. Biomed. Mater. Res.* **2002**, *65* (2), 188–195.
(31) Wohlfarth, C.; Wohlfarth, B. In: *Surface Tension of Pure Liquids and Binary Liquid Mixtures*; Lechner, M. D., Ed.; Springer, New York, 1997.
(32) Coradin, T.; Livage, J. *Acc. Chem. Res.* **2007**, *40*, 819–826.
(33) Chronakis, I. S.; Ramzi, M. *Biomacromolecules* **2002**, *3*, 793–804.
(34) Nie, H.; He, A.; Zheng, J.; Xu, S.; Li, J.; Han, C. C. *Biomacromolecules* **2008**, *9*, 1362–1365.
(35) Kongkhlang, T.; Kotaki, M.; Kousaka, Y.; Umemura, T.; Nakaya, D.; Chirachanchai, S. *Macromolecules* **2008**, *41*, 4746–4752.
(36) Kang, Y.-M.; Kim, K.-H.; Seol, Y.-J.; Rhee, S.-H. *Acta Biomaterialia* **2009**, *5*, 462–469.
(37) Van de Witte, P.; Dijkstra, P. J.; van den Berg, J. W. A.; Feijen, J. *J. Membr. Sci.* **1996**, *117*, 1–31.
(38) Allo, B. A.; Rizkalla, A. S.; Mequanint, K. *Langmuir* **2010**, *26* (23), 18340–18348.
(39) Kakade, M. V.; Givens, S.; Gardner, K.; Lee, K. H.; Chase, D. B.; Rabolt, J. F. *J. Am. Chem. Soc.* **2007**, *129*, 2777–2782.
(40) Birchall, J.D. In *The Colloid Chemistry of Silica*, Bergna, H. E., Ed.; ACS Advances in Chemistry Series; American Chemical Society: Washington, D.C., 1994; Vol. 234, p 601.
(41) Swaddle, T. W. *Coord. Chem. Rev.* **2001**, *219-221*, 665–686.
(42) Li, L.; Yalcin, B.; Nguyen, B. N.; Meador, M. A. B.; Cakmak, M. *ACS Appl. Mater. Interfaces* **2009**, *1* (11), 2491–2501.
(43) Li, P.; Ohtsuki, C.; Kokubo, T.; Nakanishi, K.; Soga, N.; Nakamura, T.; Yamamuro, T. *J. Am. Ceram. Soc.* **1992**, *75* (8), 2094–2097.
(44) Cho, S. B.; Miyaji, F.; Kokubo, T.; Nakanishi, K.; Soga, N.; Nakamura, T. J. *Biomed. Mater. Res.* **1996**, *32*, 375–381.
(45) Kokubo, T.; Takadama, H. *Biomaterials* **2006**, *27*, 2907–2915.
(46) Heinemann, S.; Heinemann, C.; Bernhardt, R.; Reinstorf, A.; Nies, B.; Meyer, M.; Worch, H.; Hanke, T. *Acta Biomater.* **2009**, *5*, 1979–1990.
(47) Mann, S. *Nature* **1998**, *332*, 119–124.
(48) Dorozhkina, E.; Dorozhkin, S. V. *Colloids Surf., A* **2002**, *210*, 41–48.
(49) Lee, J. S.; Lu, Y.; Baer, G. S.; Markel, M. D.; Murphy, W. L. *J. Mater. Chem.* **2010**, *20*, 8894–8903.
(50) Hench, L. L. *J. Am. Ceram. Soc.* **1998**, *81*, 1705–1728.
(51) Radin, S.; El-Bassyouni, G.; Vresilovic, E.J; Schepers, E.; Ducheyne, P. *Biomaterials* **2005**, *26* (9), 1043–1052.
(52) Navarro, M.; Aparicio, C.; Charles-Harris, M.; Ginebra, M. P.; Engel, E.; Planell, J. A. In *Advances in Polymer Science: Ordered Polymeric Nanostructures at Surfaces*; Vancso, G. J., Reiter, G., Eds.; Springer-Verlag: Berlin, 2006; Vol. 200, pp 209−231.